



Mechanical & Microstructural Analysis of Armor Steel Welded Joints

Tekin Özdemir¹

¹National Defence University, Turkish Military Academy, Department of Mechanical Engineering, Ankara, 06380 TURKEY

Başvuru/Received: 27/11/2018

Kabul / Accepted: 30/09/2019

Çevrimiçi Basım / Published Online: 31/12/2019

Son Versiyon/Final Version: 31/01/2020

Abstract

One of the main construction materials used in armor vehicles is Mil-A 46100 Armor Steel. The importance of the material arises from its mechanical properties such as hardness and explosive protection capability. MIG (Metal Inert Gas) welding technique is principally based on welding metals via electric arc where the arc is continuous between metals and welding wire. In case welded metals are steel based materials, O₂ and CO₂ are added in protective gases in order to prevent unexpected welding defects. In MIG welding applications, the amount of ferrite in the chemical structure of the armor steel may result in some unexpected affects due to its decreasing characteristic on ductility and toughness. The welding wires used in MIG operations may exhibit different fracture characteristics; as some specimen show ductile fracture characteristics, the rest may show brittle. Charpy Impact Test is one of the effective tests to determine the impact energy and the fracture times of welded metals. In this study, it is aimed to determine the relations between micro-structural results and fracture times of the welded parts of Mil-A 46100 steels via MIG applications.

Key Words

“MIG, Welding, Fracture energy, Brittle, Ductile”

1. Introduction

Armor steels are more keen to be welded compared to any other type of metals. Besides this, thanks to those good mechanical properties, they are preferred in armor vehicle construction. Joining of high strength armour steel plate developed for lighter armour vehicles using both austenitic and ferritic type of electrode/filler wire could show inferior ballistic performance of the welds. Armour grade quenched and tempered (Q & T) steel closely conforming to AISI 4340 is primarily used for construction of military and non-military vehicles, because of their high energy absorbing properties. The ballistic requirement of Q & T steels used for armour application requires high strength, greater notch toughness and high hardness. The effect of heat-input on the heat affected-zone (HAZ) softening in Q & T steel and width of the soft zone and, in turn, its influence on hardness and ballistic performance was investigated by Reddy and Mohandas. (M. Balakrishnan et al., 2013)

Combination of hard facing electrode and softer Austenitic Stainless Steel electrodes, though provided improved ballistic performance, might not satisfy main design criteria such as strength and toughness due to non-homogeneous microstructure of weld metal. In order to satisfy improved ballistic performance as well as other design parameters, it is highly desirable to develop coated electrode which will attribute more homogeneous microstructure in weld metal similar to high strength armour steel plate. (A.K. Pramanick et al., 2016) Also known as armor steel, these materials are generally used as armored combat vehicles. Armored vehicles have large number of joining methods due to their complex structure. Therefore, different welding methods are widely used in joining processes in combat and logistics vehicles. Choosing correct welding method and parameters is crucial in field performance of armored vehicles. (Sarsilmaz et al., 2017) Also some scientists used various techniques to measure hardness and impact energy of welded area and gives especially results of Split-Hopkinson tests. (Falkenreck et al., 2017)

Some scientists evaluated the crystallographic texture, defined as the distribution of orientation of crystals (or grains), to gauge the deformation and microstructural evolution of ARMOX 500T armour plates at elevated strain rates. Using neutron diffraction, the authors examined a number of specimens deformed at room temperature and high strain rates and contrasted these with equivalent samples deformed quasi-statically. Since crystallographic texture can play a part in the armour's ballistic response the authors were able to observe a rate dependent textural development, with the strengthening of the rolling α -fibre. The hot rolling process used in the manufacture of these steels leads to a through thickness texture variation that leads to an asymmetric transitional texture in the strain regime (1–2%) but with increased strain a symmetric texture develops irrespective of the strain rate, albeit with different intensities. (M. Saleh et al., 2018) An investigation on welding high strength armor steels with austenitic filler material using Gas Metal Arc Welding (GMAW) process, armor plates conforming to MIL A 46100 standard were prepared with six different groove angles using 307 Si austenitic stainless steel electrode. Welded test specimens were subjected to tensile testing and microhardness measurements in three zones (fusion zone, heat affected zone and base metal zone) were recorded. Comparing the results obtained from both tensile testing and microhardness measurements, the optimum groove angle to result in the highest mechanical properties is determined. They used MIL A 46100 armour steel, using Gas Metal Arc Welding process and six different groove angles using 307 Si austenitic stainless steel electrode. Welded test specimens were subjected to tensile testing and microhardness measurements. Comparing the results obtained from both tensile testing and microhardness measurements, the optimum groove angle to result in the highest mechanical properties is as 48° (Kurt et al., 2016) In a welding application, based on the results obtained in a previous study by using E11018M, a ferritic filler exhibiting similar chemical and mechanical properties was selected. The final selection relied on ER100S-1 wire based on commercial availability and the fact that ESAB trademarked filler is the only one that meets the requirements of the MIL-E-23765/2 standard. (Robledo et al., 2011) MIL-STD-1185 is also important for our study - Welding High Hardness Armor designates standards for MIL-A 46100 armour steel. (Military Specification Armor Plate, 1983)

In an MSc thesis about MIL-A 46100 armour steel, the mechanical properties are measured as hardness 510 HV, and toughness 43 Joules (J). Then some heat treatment applications are conducted on the steel. As the tempering heat rises, they saw that the hardness decreases. Also they saw the martensitic phases in all their heat treatment levels in the microstructures. After welding operation, they noticed that there are still some martensitic zones in the welded area despite the high heat transfer during the welding operation. Thereafter the welded and heat-treated parts are put under an impact test. As a result, they found that the heat-treated specimen has a toughness of 60 J, whereas the original specimen 46 J. (Merzalı, 2013) The impact toughness and elongation rate of MI 307 Si welding wire is 80 J and %40 according to a proceeding. (Çelik Ç., XI. Welding Congress) The most known and most widely used steel armour plates are ARMOX steels by Swedish company SSAB Oxelosund. The steels have lean chemical composition which simplifies welding. Carbon equivalent (1) of these steel is relative low (0.6-0.7), therefore they have very good weldability. $CEV = C + Mn/6 + (V + Mo + Cr)/5 + (Cu + Ni)/15$ [%]. However, their welding is problematic due to heat influence during welding process. Armox steels have high strength, hardness and good toughness. The steels acquire these specific properties by application of thermo-mechanical treatment (TMT) and therefore the producer recommends do not exceed the temperature circa 200°C during their secondary processing as is welding. The reason of degradation of mechanical properties during ARMOX 500 steel welding are changes in microstructure. The original (un-affected) microstructure consists of very fine-grained heterogeneous sorbitic structure obtained as a result of thermo – mechanical treatment. This structure provides high strength, toughness and hardness required from this kind of steels. (Barényi et al., 2012)

In an Impact test, first the energy amount to break the specimen is designated as the impact strength. In those applications, the Pendulum is the best solution. The pendulum has a G mass and h height at the beginning having a potential energy of Gxh . When the Pendulum is freed at that height, it moves and breaks the specimen, then goes back to the h_1 position, which is near to the initial position. Thus, the potential energy left on the pendulum is Gxh_1 . The difference between the potential energies when the pendulum first touches the specimen, and after the break is the energy amount enough to break that specimen. In other words, this energy

difference is described as the Impact Resistance. In a study, Ramor 500 armor steels which are used in armored combat vehicles were welded by MIG (Metal inert gas) welding method. 307 Si MIG welding wire was used as an additional metal which is proposed for MIG welding of armor steels. The effect of welding groove type on metallurgical and mechanical properties was investigated in experimental studies. Three different conditions, which were included Y, X and Z were selected as welding groove. (Kara et al., 2016)

Ramor 500 armor steels which are used in armored combat vehicles were welded by MIG (Metal inert gas) welding method. 307 Si MIG welding wire was used as an additional metal which is proposed for MIG welding of armor steels. The effect of welding groove type on metallurgical and mechanical properties was investigated in experimental studies. Three different conditions, which were included Y, X and Z were selected as welding groove. The welding grooves were shaped by using the milling method. The microstructures of the weld regions were examined by optical microscope, SEM, EDS and XRD. Mechanical properties of the specimens were determined by microhardness tests and impact tests. As a result, the effect of design of welding groove on welding strength was identified for joints of armor steels. (Thora et al., 2017) In a study it is shown that the hardness in the heat affected material is not constant along the path. This hardness is considered for the heat treatment. Maximum hardness is located where the maximum deformation will occur on welded joints under dynamic loads due to high geometrical stress concentration. The aim of heat treatment is to obtain tensile specimens with mechanical properties close to those of a HAZ obtained by welding and not to recreate there a local complex thermal cycle induced by the welding process. These specimens are used to characterize the HAZ material dynamic behavior. (J. Carrier et al., 2017)

The influence of different welding speeds and rotary speeds on the formation and mechanical properties of friction stir weld joints of armor grade aluminum alloy were investigated in a study. The weld joints were characterized by bend tests, micro-hardness tests, tensile tests, optical and scanning electron microscopies. Mechanical properties (i.e., micro-hardness, ultimate tensile strength and elongation to fracture) increased with the increase in rotary speed or decrease in welding speed. The effect of welding speed on micro-hardness of heat affected zones was more profound than the rotary speeds. The welding speeds and rotary speeds influenced the mechanical properties and their effects on various mechanical properties of the friction stir welded joints can be predicted with the help of regression models. (C. Sharma et al., 2017) It is found in a test that, the best combination of heat treatment together with metal chemical composition and cleanliness in steel imparts acicular martensite microstructure which is responsible for superior dynamic fracture toughness compared to the welded joints. Also, the dynamic fracture toughness of the manually welded joint is higher than that of the automatically welded joint owing to the presence of a circular ferrite microstructure in the weld metal region. (G Magudeeswaran et al., 2010)

R. Lezcano et al. (2009) proves that; when making welding joints, small discontinuities, voids and other defects cannot be absolutely avoided and the heterogeneity of the own joint along with the presence of residual stresses may be taken into account in order to prevent failures and to assure the integrity of the whole component or structure. One of the key factors for understanding the fracture behaviour of any welded structure containing cracks is the heterogeneity of the joint. In an ideal weld, where a crack is contained within the weld metal and can grow parallel to the weld metal-base metal interface, assuming that the effect of the heat affected zone is negligible. For the welded structures are subjected to large plastic deformation, due to the interaction between weld strength mismatch and weld geometrical feature, a more complicated local stress status and plastic strain concentration can be observed in the welded zones, which make ductile cracks tend to occur primarily at and near the welds, affecting the final failure mode and performance of welded structures. (Hao Wang et al., 2018) Kang et al. (2015) investigated the ductile fracture behaviours of welded joints and small welded connections through experimental and numerical analyses, proposing the ductile fracture models and related parameters of different welded zones.

According to the study conducted by Hongchao Guo et al. (2018) the welded joint of steel structure is prone to occur fatigue fracture under dynamic loads. In this paper, an experimental study on the fatigue performance of base material, butt weld, and cross fillet weld of high-strength steels were investigated. The S-N curve was fitted, and the corresponding fatigue life was predicted. Results show that the base material of high-strength steel possess high fatigue resistance. Also, a quantitative analysis on fatigue fracture was conducted on the basis of fatigue damage theory, and the fatigue crack propagation law was disclosed on the basis of fracture morphology. The crack propagation law before instant fracture is consistent with damage development, and the fatigue striation width increases gradually with damage development. The fast crack propagation stage accounts for a small proportion in the fatigue life, thereby indicating that this stage is insufficiently developed. The fracture toughness of two types 316LN welded joints in different orientations at 300 K and 623 K in air was investigated. The tests were conducted using single specimen method, where J-R curves and fracture toughness values were obtained. Microstructure of the specimens were characterized before and after the test. Results show that 2GT welded joint exhibits higher toughness as compared to 5GT welded joint, and orientation has slight effect on the fracture toughness. Moreover, the fracture toughness drops remarkably with the increase of temperature. Wenhua Gao et al. (2017) Yonghe Yang et al. suggest that; the microstructures, mechanical properties and fracture toughness of the materials in different locations of the welded joint of the X80 pipeline steel were studied at room temperature. Elastic-plastic fracture toughness testing of crack tip opening displacement (CTOD) and J-integral of the welding materials and base material were conducted. A new non-contact double-clip gauge measuring system was developed and used in the fracture toughness tests. It was observed the fusion zone (FZ) was the fracture risk zone of the X80 steel weldment; and the occurrence of hard-brittle martensite-austenite (M-A) constituents was a significant because of welding hardening and embrittlement.

2. Material Specifications and Technical Data

2.1. MIL-A 46100 Armor Steel Mechanical Properties

The Chemical Compound and Mechanical Properties of MIL-A 46100 Steel are shown on the Table1-2. As seen on the tables the armour steel has dominantly Carbon in the chemical compound, and the Charpy Impact energy level of 28 J.

Table1. Chemical Compound of MIL-A 46100 Steel (Robledo at el., 2011)

Element	Wt. %	Element	Wt. %
C	0.284	Sb	0.001
V	0.007	Ti	0.031
Al	0.020	P	0.010
Sn	0.008	S	0.002
Cu	0.177	Pb	0.005
Cr	0.300	Ni	0.192
Si	0.534	Mo	0.243
Mn	0.899	Fe	Balance

Table 2. Mechanical properties of MIL-A-46100 steel plates (Robledo at el., 2011)

Property [Units]	Value
Tensile Strength [MPa]	1690
Elongation [%]	25
Charpy V-Notch @ -20 °C [J]	28
Hardness [Hv]	525

2.2. Weld Groove Types Used in the Experiments

V and Double V (X) grooves are opened with a 30° angle on each plate before welding operation in order to make a comparison between the weldings. The welding has been performed along with X direction.

2.3. Welding Wire Types & Mechanical Properties

The following two kinds of welding wires are chosen because they have enough capability for armour and hardfacing applications as seen on Tables 3-4. MI 307 Si wire is an Austenitic stainless steel wire electrode for GMA (MIG/MAG) welding of dissimilar steels, difficult to weld steels, armour plates, high manganese steels, rails, crossovers. Weld metal has a high degree of corrosion resistance and resistant to operating temperatures up to 300°C and non-scarring up to 850°C.

Table 3. Chemical Compound of MI 307 Si wire

Element	C	Si	Mn	Cr	Ni
Wt. %	< 0.20	0.65 - 1.00	4.50 - 7.50	17.00 - 20.00	7.00 - 10.00

FCH 330 wire is gas shielded flux cored wire which is developed for hardfacing of parts subjected to metal-to-metal friction (abrasion) and medium degree impacts. Due to its very tough and crack resistant weld metal, it is also used for buffer layer applications. As the weld metal has medium degree hardness it can be machined by chip forming and flame or inductive hardening is possible. Interpass temperature should not exceed 250°C during welding.

Table 4. Chemical Compound of FCH 330 wire

Element	C	Si	Mn	Cr	Fe
Wt. %	0.14	0.40	1.10	1.25	Remain

3. Test Preparation And Methodology

3.1. Material & Sample Preparation

The MIL-A 46100 plates are welded using MI 307 Si wire and FCH 330 wire respectively via XMS 44 Welding machine. The wire feeding speed is designated as 8 m/min. The welding current was approx. 220 amperes under 30 volts of voltage. The specimens are machined via modern 3 and 5-axis milling machines. The welded armour plates were sliced into 10 mm parts in order to prepare Charpy test specimen as seen on pictures 1-2.



Pic.1. Welded part with X groove



Pic.2. Charpy Test Specimen

3.2. Weld Groove Types Used in the Experiments

V and Double V (X) grooves are opened with a 30° angle as seen on Fig.1, on each plate before welding operation in order to make a comparison between the weldings. The welding was performed along with X direction as seen on Fig.2.

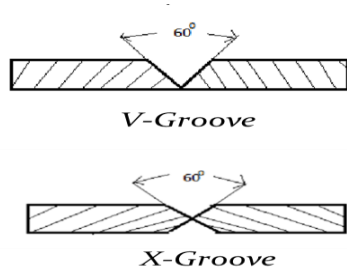


Fig.1. V and X grooves

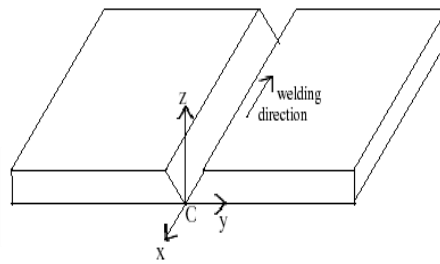
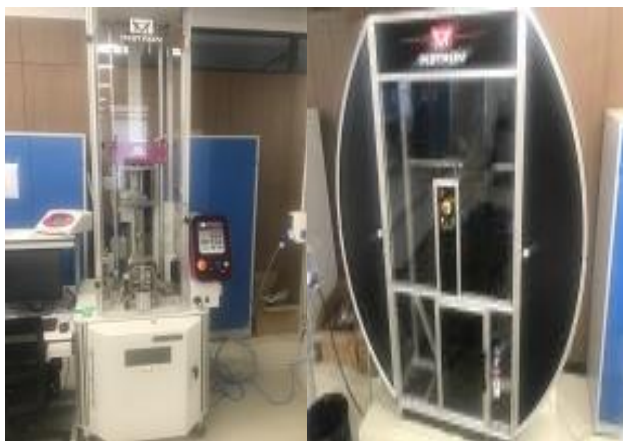


Fig.2. Welding direction

After preparation of specimen, the Charpy Impact Energy tests were conducted on INSTRON CEAST 9350 and INSTRON Pendulum devices seen on Pic.3. Impact tests were conducted on the specimen with X and V grooves extracted from welded parts at STP. The standard for welded parts for impact test is described on BS EN 875 test standards document. Each energy value obtained is the arithmetic average of three tests. Following tests, the surface morphology was inspected via JEOL SEM device seen on Pic.4. According to the test standards document, the notch depth is designated as 1 mm at the center of the sample, while the sample having the dimensions of 10x10x55 mm.



Pic.3. Charpy impact & pendulum test devices



Pic.4. JEOL SEM device

4. Scientific Background

Fracture toughness criteria, Charpy impact toughness (K_{IC}) for each sample is used to validate crack propagation and fracture type. Charpy impact toughness values are calculated from charpy impact energy by using J integration of the crack length Δa expressed as below. (Kraft, J. M.,1964) (Ozdemir T. At et al., 2015)

Charpy impact energy and fracture toughness are given;

$$J = C. \Delta a^p \tag{1}$$

Here C is compliance and defined by geometry of charpy specimen (a_0, B_0, w) as follows,

$$C = \left(\frac{2}{p}\right)^p \cdot \frac{\eta(a_0)}{B_0 \cdot (w-a_0)^{p+1}} \cdot W_t^p \cdot W_m^{1-p} \quad (2)$$

Where W_t is entire fracture energy, W_m is state energy achieved at maximum force,

p and $\eta(a)$ are parameters defined by

$$p = \frac{3}{4} \cdot \left(1 + \frac{W_m}{W_t}\right)^{-1} \quad (3)$$

$$\eta(a) = 13,81 \cdot (a/w) - 25,12 \cdot (a/w)^2 \quad (4)$$

$\frac{W_m}{W_t} = n$ Here n is strain-hardening coefficient approximately equal to ductility (A_f) according to Kraft et al.

$$J = \left(\frac{2}{p}\right)^p \cdot \frac{\eta(a_0)}{B_0 \cdot (w-a_0)^{p+1}} \cdot W_t \cdot A_f^{1-p} \cdot \Delta a^p \quad (5)$$

Here $W_t = KV$ and, KV is impact energy.

For plane strain conditions fracture toughness can be defined as follows;

$$K_{IC} = \left(J \cdot \frac{E}{(1-\nu^2)}\right)^{0.5} \quad (6)$$

This equation is suitable for our Charpy Impact Energy tests.

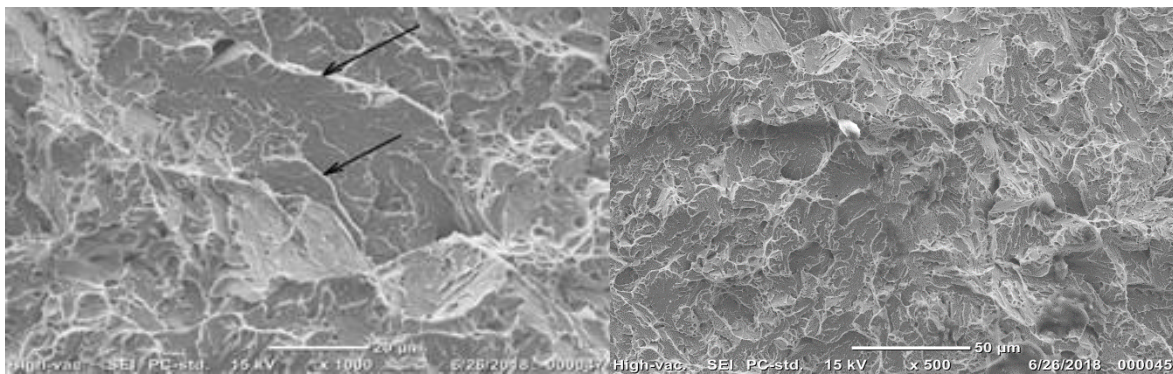
5. Results

5.1. Welding Results

In the overall inspection of all fractured surfaces; the similarity in fractured surface morphologies of all specimen shows that the welding parameters are applied properly for the process. Welding wires both give satisfactory results, but 307 Si wire provides with better mechanical properties compared to FCH 330 wire. In welding application of MIL-A 46100 Armour steel; groove angle, wire feeding speed, voltage and currency are all important parameters for effective welding operations. Groove angle is effective for MIG welding as 60° .

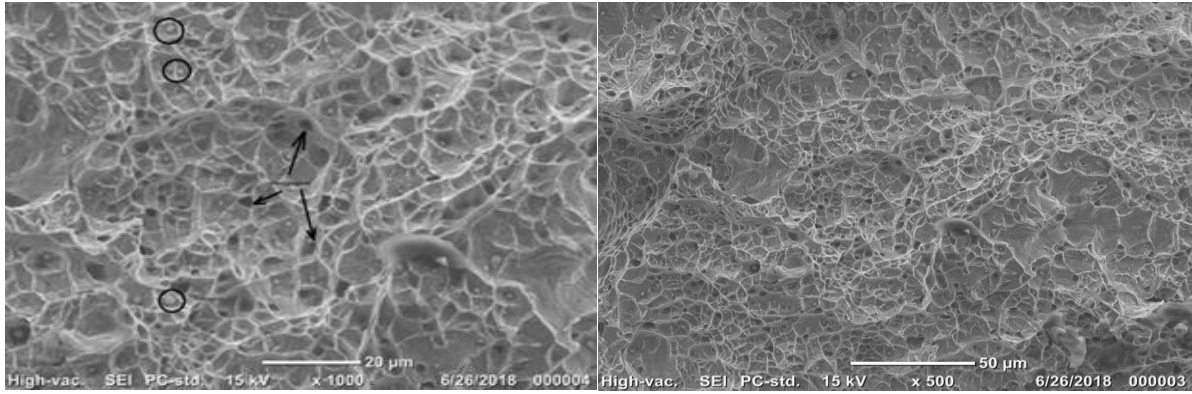
5.2. Microstructural Analysis

No critical defects are seen on Picture 3.a,b showing the microstructure of welded parts. Fibrous scenes seen on the SEM photos mean that the fracture type on the inspected areas are like ductile cleavage, depending on the weld wires' mechanical properties. According to the micro-granular (grain-sizes in 500x and 1000x photos) morphology; the injected heat, welding speed, wire feeding speed, weld groove and the mechanical properties of welding wires have dominant effect on the quality of the weldings. Another finding pertaining to the brittle cleavage of sample welded with MI307 Si is that; there are microporous areas on the inspected zone. The porous scenes on the fracture are dominant and they are very small structures, which means that the fracture happens very quickly.



Pic.5. a,b Microstructure of welded samples with FCH 330 wire

The fracture seems to happen like cleavage type fracture because; fracture first initiates from the grains, then accelerates along a plane, damage in one plane triggers the others along an axis and the damage widens straightly. There is an example of this kind of cleavage seen on the pic.6 a,b below.



Pic.6. a,b Microstructure of welded samples with MI307 Si wire

5.3. Impact Energy

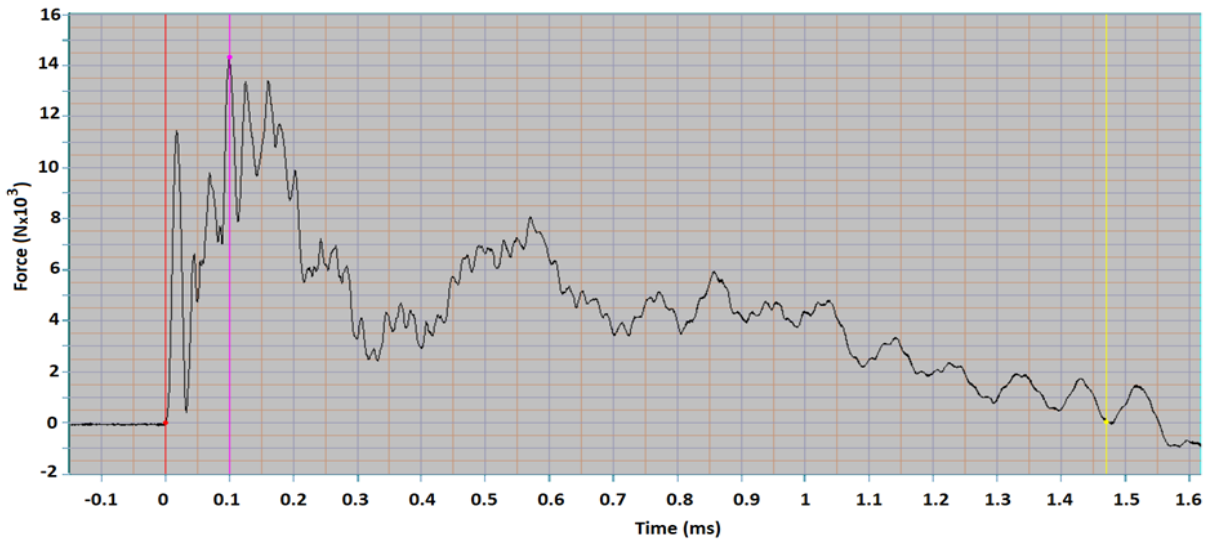
As seen on the Table 5 below, HAZ of the weldings has satisfactory impact energy levels, V grooved specimens show better resistance to impact energy compared to the X groove. Compared to the other scientific studies mentioned in the introduction phase of this study, the results are similar and in accordance with each other.

Table 5. Charpy Pendulum & Impact Energy of Welded Parts

# Sample	Weld Filler	Groove	Charpy Pendulum Energy Absorbed (J)	Charpy Impact Energy Absorbed (J)
I	MI 307 Si	X	50.22	29.53
II	MI 307 Si	V	87.12	94.26
III	FCH 330	X	18.69	29.94
IV	FCH 330	V	46.60	41.37

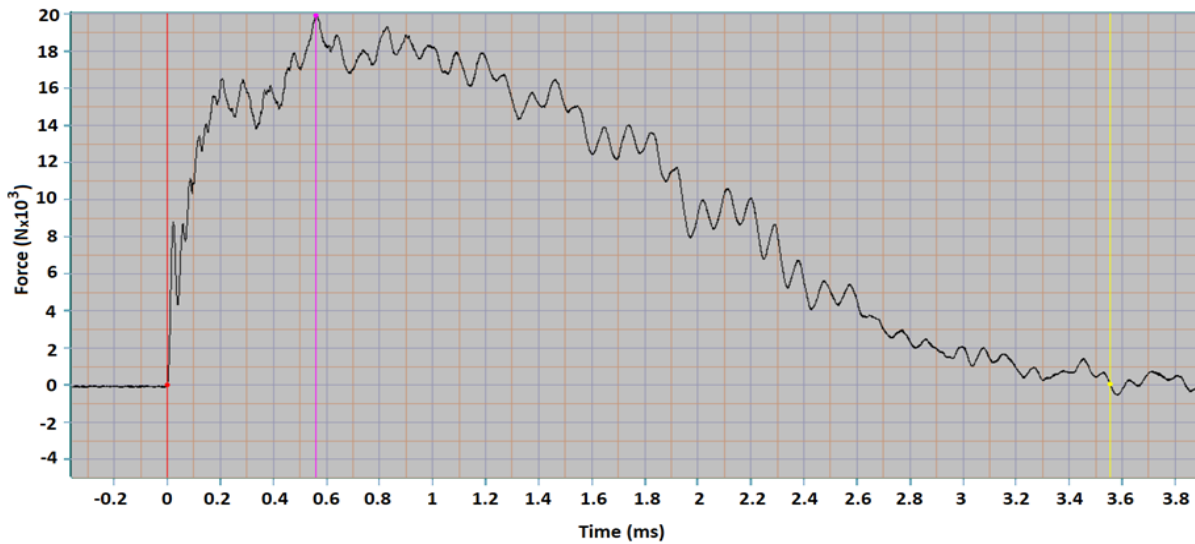
5.4. Fracture mechanical analysis

The following data is obtained directly from Instron CEAST 9350 device.



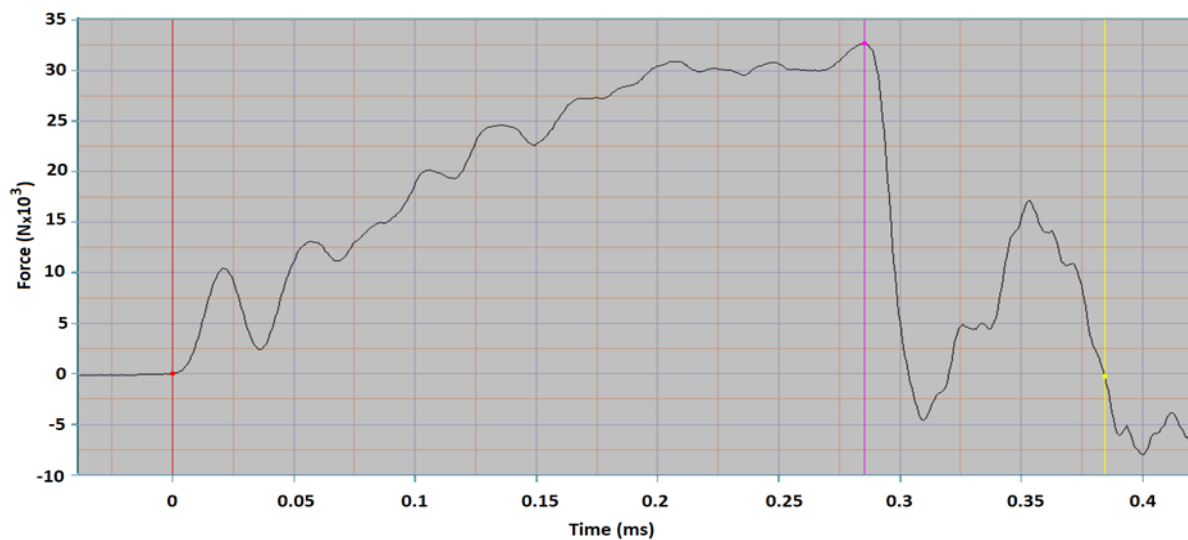
Graph 1. Force-time fracture graph of sample I

On graph 1, it is explicitly seen that, the fracture happens very quickly at 0.1 millisecond (ms) via 14 kN force. The groove type of sample I is X, which is not preferable compared to V groove and the fracture is brittle compared to the other samples. The fracture curve exhibits a deceleration until the time 1.5 ms where the load becomes 0 kN. This means that the cleavage started and ended in a very small time interval, which is a basic behaviour of brittle fracture of metals. Also, we have to mention that, the X grooved sample has very little impact absorb capacity compared to the V grooved sample. This sample's impact resistance is smaller than sample II as seen on Table 5.



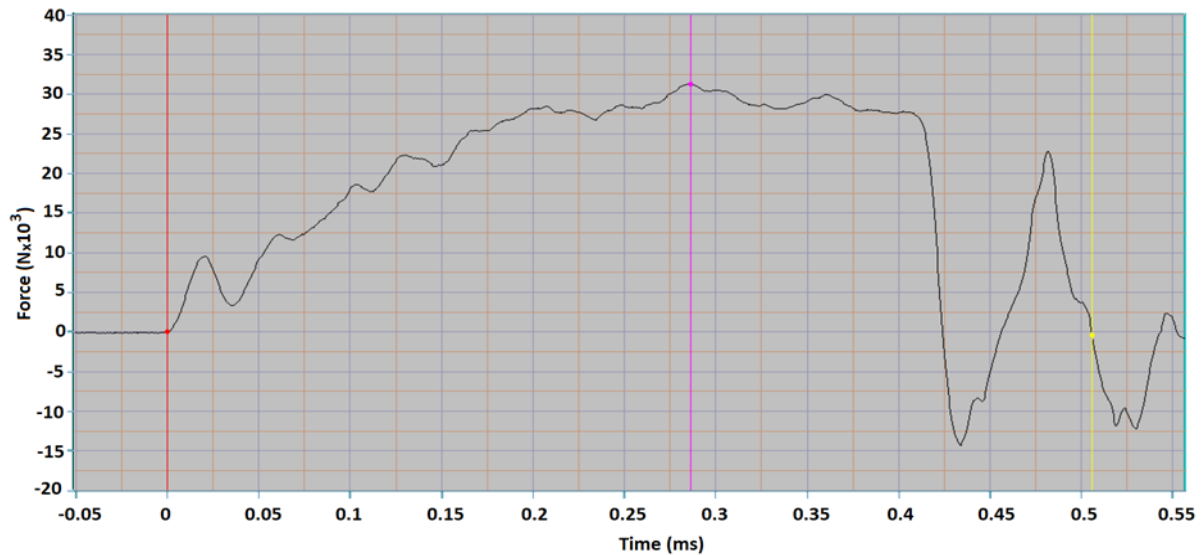
Graph 2. Force-Time fracture graph of sample II

On graph 2, it is seen that, the fracture happens quickly at 0.58 milisecond (ms) via 20 kN force, but this cleavage lasts longer. The groove type of sample II is V, which is more preferable than X groove in armor weldings. The fracture is again brittle compared to the samples III, IV. The fracture curve exhibits more moderate deceleration than sample I, until the time 3.5 ms where the load becomes 0 kN. This means that the cleavage started and ended in a very small time interval, which is also a basic behaviour of brittle fracture of metals. Sample II has more impact resistance than sample I, owing to V groove type and weld filler material's carbon ratio, as seen on Tables 3,5.



Graph 3. Force-Time fracture graph of sample III

On graph 3, the scheme of fracture changes completely shifting from brittle fracture to ductile. The fracture happens quickly at 0,28 milisecond (ms) via 30 kN force. The groove type of sample III is X, which is less preferable than V groove in armor weldings. The fracture is ductile compared to the samples I, II. The fracture curve exhibits a deliberate deceleration until the time 0.38 ms where the load becomes 0 kN. This means that the cleavage started and ended in a very small time interval, but because of the X groove which has less impact energy absorb capacity than V groove, the fracture starts in a ductile form but results in a brittle form.



Graph 4. Force-Time fracture graph of sample IV

On graph 4, the scheme of fracture is completely ductile. The fracture happens quickly at 0,28 milisecond (ms) via 30 kN force. The groove type of sample IV is V, which is more preferable than X groove in armor weldings. The fracture is ductile compared to the samples I, II and III. The fracture curve exhibits a resistance to impact energy between 0.28 to 0.43 ms. After 0.45 ms, the impact energy beats the resistance of the sample and there happens a deliberate deceleration at 0.45 ms where the load becomes 0 kN. This means that the cleavage started and ended in a very small time interval, the fracture results in ductile form in general.

6. Conclusions

Welding parameters used in the process are good enough to meet the ballistic requirements for Mil-A 46100 armor steel in the operational area. Welding wires both FCH 330 and MI 307 Si give satisfactory impact energy results, but 307 Si wire provides with better mechanical properties to the welding, due to having more carbon ratio in the compound. HAZ of the conducted weldings have satisfactory impact energy absorption levels compared to the mechanical properties shown on Table 2. V grooved samples exhibit better impact resistance compared to the X grooved ones, since the HAZ of the former has better Welding quality compared to the later. Groove angle, wire feeding speed, voltage and current are important parameters for effective welding operations in Welding applications of armour steels. Groove angle effective for MIG Welding in armor steel Mil-A 46100 is found as 60°, via the comparison of the results of the other welding results conducted by other groove angles. There are porous areas on the inspected fracture surfaces, which means that the fracture occurs very quickly owing to the weld wires' chemical composition, and depending on the impact absorption capacity of the welded area. Fibrous scenes are seen on the SEM photos especially on samples welded using FCH 330 wire, meaning that the fracture type is less brittle than the ones welded with MI307 Si wire. In terms of fracture times of the samples; fractures in the armour steel welded joints may exhibit brittle or ductile characteristics depending on the groove types, carbon ratio in the compounds, and weld filler used in the welding operations. In the overall scheme of Charpy tests conducted on the samples chosen, the cleavage in the welded joints are very quick and mostly brittle owing to the carbon ratio in the weld wires' compounds.

References

- Balakrishnan M., Balasubramanian V., Reddy G. M. (2013), Effect of hardfaced interlayer thickness on ballistic performance of armour steel welds, *Materials and Design*, 44 (2013) 59–68.
- Barényi I., Híreš O., Lipták P. (2011), International, Degradation Of Mechanical Properties Of Armoured Steels After Its Welding, Conference Of Scientific Paper AFASES 2011, Brasov, 26-28 May 2011.
- Carrier J., Markiewicz H., Lebaillif, Leconte, Naceur, (2017) Influence of the heat affected zone on the dynamic behavior of a welded joint of armoured steel, *International Journal of Impact Engineering* 104 (2017) 154-163
- Çelik Ç., IX. Kaynak kongresi Ulusal kongre ve sergisi bildiriler kitabı zırh çeliklerin kaynağında kaynak ağzı geometrisi ve ilave tel optimizasyonu, (Pg.89-94).
- Gao W., Chen K., Guo X., Zhang L. (2017) Fracture toughness of type 316LN stainless steel welded joints, *Materials Science & Engineering A* 685 (2017) 107–114.
- Guo H., Wan J., Liu Y., Hao J., Experimental study on fatigue performance of high strength steel welded joints, *Thin-Walled Structures* 131 (2018) 45–54.

- Kang L., Ge H., Kato T., Experimental and ductile fracture model study of single Groove welded joints under monotonic loading, *Engineering Structures* 85 (2015) 36–51.
- Kara S., Korkut M.(2012), Zırhlı Muharebe Araçlarında Kullanılan Zırh Plakalarında Kaynak Sonrası Isıl İşlemin Birleşim Mukavemetine Etkisinin Araştırılması, *The Journal of Defense Sciences*, November 2012, Volume 11, Issue 2, 159-171, ISSN: 1303-6831.
- Kelami Ş.M., Emre M.C., (2013) Zırh çeliklerinde kaynak sonrası ısı tesiri altında kalan bölgenin özelliklerinin ısı işlem ile iyileştirilmesi, MSc Thesis, Istanbul Technical University Science and Technology Institute, June 2013.
- Kraft, J. M., Correlation of plane strain toughness with strain-hardening characteristics of a low, medium, and a high strength steel. *Applied Materials Research* 3, (1964).
- Kurt S., Evci C., Işık H., Işık M.S.(2016) Farklı Kaynak Ağız Açılarının 307Si Elektroduyla Kaynak Edilmiş Mil-A 46100 Zırh Çeliğinin Mekanik Özelliklerine Etkisinin İncelenmesi, *Çukurova University Journal of the Faculty of Engineering and Architecture*, 31(ÖS 1), pp. SI 155-SI 162.
- Lezcano R., Rodríguez C., Peñuelas I., Betegón C., Belzunce F.J., (2009), Effect of mechanical mismatching on the ductile-to-brittle transition curve of welded joints, *Engineering Failure Analysis* 16 (2009) 2576–2585.
- Magudeeswaran G., Balasubramanian V., Reddy G. M. (2014) Effect of welding processes and consumables on fatigue crack growth behaviour of armour grade quenched and tempered steel joints, *Defence Technology*, 10 (2014) 47-59.
- Ozdemir T., Eruslu O.S., Finite element modelling of crackable connecting rods at fracture splitting process, (2015) *Mechanika* Volume 21(2): 85–90.
- Pramanick A.K., Das H., Reddy G.M., Ghosh M., Das G., Nandye S., Pal T.K. (2016) Development and design of microstructure based coated electrode for ballistic performance of shielded metal arc welded armour steel joints, *Materials and Design*, 103 (2016) 52–62.
- Robledo D.M., Gómez J.S., Barrada J.G. (2011) *Dyna*, ano 78, Development Of A Welding Procedure For Mil A 46100 Armor Steel Joints Using Gas Metal Arc Welding, *Medellín Agust 2011*, Nro. 168, pp. 65-71, ISSN 0012-7353.
- Saleh M., Kariem M., Luzin V., Topplerf K., Li H., Ruan D. (2018) High strain rate deformation of ARMOX 500T and effects on texture development using neutron diffraction techniques and SHPB testing, *Materials Science & Engineering A*, 709 (2018) 30–39.
- Sarsilmaz F., Kirik I., Batı S.(2017), Microstructure and mechanical properties of armor 500/AISI2205 steel joint by friction welding, *Journal of Manufacturing Processes*, 28 (2017) 131–136.
- Sharma C., Upadhyay V., Dwivedi D. K., Kumar P., Mechanical properties of friction stir welded armor grade Al–Zn–Mg alloy joints, *Trans. Nonferrous Met. Soc. China* 27(2017) 493–506.
- Thora E., Falkenreck M.K., Böllinghaus T.(2017), Dynamic compressive behaviour of weld joints, *Materials Science & Engineering A*, 702 (2017) 322–330.
- US Patent, Military Specification Armor Plate, Steel, Wrought, High-Hardness MIL-A-461OOD(MR), 16 May 1988, Superseding, 13 June 1983.
- Wang H., S. Xu, Wang Y., Li A., Effect of pitting degradation on ductile fracture initiation of steel butt-welded joints, *Journal of Constructional Steel Research* 148 (2018) 436–449.
- Yang Y., Shi L., Xu Z., Lu H., Chen X., Wang X., Fracture toughness of the materials in welded joint of X80 pipeline steel, *Engineering Fracture Mechanics* 148 (2015) 337–349.